Angewandte Chemie
Eine Zeitschrift der Gesellschaft Deutscher Chemiker

Supporting Information

# Electrostatics and Intrinsic Disorder Drive Translocon Binding of the SRP Receptor FtsY

*Nils-Alexander Lakomek*[+],* *Albena Draycheva*[+], *Thomas Bornemann, and Wolfgang Wintermeyer**

anie_201602905_sm_miscellaneous_information.pdf

## Materials and Methods

**Expression and purification of FtsY.** FtsY and FtsY-A207 were expressed from a pET SUMO vector with N-terminal $His_6$-tag in *E. coli* BL21(DE3)pLys cells (Invitrogen) for 2 hours at 37°C. Isotope labeling of FtsY and FtsY-A207 was performed in M9 mineral medium supplemented with $^{15}NH_4Cl$, $^{13}C$-glucose and $D_2O$ instead of $H_2O$ according to a published protocol.[1] Cells were opened in an EmulsiFlex C3 homogenizer (Avestin) in 20 mM HEPES, pH 7.5, 150 mM KCl, 20 mM imidazole, 10 % glycerol, supplemented with 0.01 % nona-ethylene glycol monododecyl ether (Nikkol). The extract was centrifuged and FtsY was purified via nickel-affinity chromatography (Roche). Contaminants were eluted with 1 M KCl and FtsY or FtsY-A207 was eluted with the same buffer containing 200 mM imidazole. FtsY or FtsY-A207 was loaded on to a HiTrap Q HP anion exchange column (GE Healthcare) in 20 mM HEPES, pH 7.5, 150 mM KCl, 10 % glycerol, 1 mM dithiothreitol (DTT) and eluted by applying a gradient of 150–500 mM KCl. The $His_6$-tag was cleaved by $His_6$-tagged Ulp1 protease for 15 hours at 4 °C; protease and His-tag were removed by nickel-affinity chromatography.

**Assembly of nanodiscs.** Empty nanodiscs and nanodiscs containing SecYEG were assembled from membrane scaffold protein, MSP1D1, and *E. coli* phospholipids (Avanti Lipids) and purified by size exclusion chromatography as described previously. [2] SecY(S111C)EG containing N-terminally His6-tagged SecE was prepared by a published protocol. [3] MSP1D1 was expressed and purified as described. [2] [4] Nanodisc concentrations were calculated from the absorbance measured at 205 nm, taking into account the respective protein content. [5] All experiments with SecYEG were performed with nanodisc-embedded SecYEG.

**Fluorescence labeling of proteins.** Protein labeling at single cysteine residues with BODIPY FL (Bpy) (the N-aminoethyl)maleimide derivative; Invitrogen), 7-diethylamino-3-((((2-maleimidyl)ethyl)amino)carbonyl) coumarin (MDCC; Invitrogen), or N-((2-(iodoacetoxy)ethyl)-N-methyl)amino-7-nitrobenz-2-oxa-1,3-diazole (NBD; Invitrogen) was performed following the protocols provided by the manufacturer. Labels were attached to cysteine residues engineered at positions 167 of FtsY-A207 (Bpy), position 26 of FtsY-A207 (NBD), or at position 111 of SecY (MDCC), The respective protein was incubated in buffer (20 mM HEPES pH 7.0, 150 mM KCl, 10 % glycerol) with a 5-fold excess of dye for 2 hours at 25°C. Unreacted dye was removed on a PD-10 desalting column operated at 4°C (GE Healthcare). Labeling efficiencies were >90%, based on absorbance measurements.

**NMR backbone assignment and secondary structure analysis.** $^{15}N^{1}H$ TROSY-HSQC spectra of $^{2}H^{15}N^{13}C$-enriched full-length FtsY (132 µM) or FtsY-A207 (135.4 µM), dissolved in buffer A (20 mM HEPES, pH 7.5, 70 mM $NH_4Cl$, 30 mM KCl, 7 mM $MgCl_2$, 10 % glycerol) with 1 mM DTT were

recorded on a 700 MHz Bruker Avance I spectrometer, equipped with TXI cryo probe, at 5°C to minimize adverse amide exchange effects. Spectral backbone resonance assignment was achieved using a suite of TROSY-based 3D backbone assignment experiments, including HNCO, HNCA, HN(CO)CA, HN(CA)CB, HN(COCA)CB. [6] Spectra were analyzed and backbone assignment was performed using the NMR Draw software package. [7] Secondary chemical shifts were analyzed using the TALOS+ software.[8]

**NMR relaxation experiments.** $^{15}$N $R_1$, $R_{1\rho}$ and {$^1$H}-$^{15}$N NOE were recorded at 600 MHz using a spin-lock RF power of 2kHz for the $R_{1\rho}$ experiment. $^{15}$N $R_2$ rates were derived from $R_{1\rho}$ and $R_1$ rates as described.[9] Hahn-echo based $R_2$ relaxation experiments were conducted at 600 and 900 MHz using TROSY-detection. Measurements were conducted at 5°C, similar as described.[10] Relaxation data were analyzed using NMR Draw and dedicated scripts. [10a] [10b]

**NMR studies of FtsY lipid and translocon binding.** Three different samples were investigated using solution NMR. $^{15}$N$^1$H TROSY-HSQC spectra were recorded at 600 MHz and 5°C, using 24 scans for each transient and a total experimental time of 5.5 h. To study lipid interactions, 18 µl of FtsY-A207 (135.4 µM) was mixed with 100µl of 34 µM empty nanodiscs [2] and 18 µl $D_2O$, resulting in a final concentration of 21.6 µM nanodiscs and 16.2 µM FtsY-A207. The reference spectrum was measured with a sample containing 25 µl FtsY-A207 (135.4µM), 100 µl of buffer, and 20 µl $D_2O$, resulting in a final concentration of 22 µM FtsY-A207. Resonance intensities of the reference sample were scaled according to the difference in FtsY-A207 concentration (22 µM versus 16.2 µM). To study interactions of FtsY-A207 with the translocon, 25 µl of 235 µM FtsY-A207 were mixed with 100 µl of 44 µM SecYEG and 20 µl $D_2O$, resulting in a final concentration of 22 µM FtsY-A207 and 30 µM SecYEG. Resonance intensities were compared to the reference sample.

**Error analysis of NMR data.** The error on spectral intensities was derived from the noise level versus signal intensity using dedicated NMRPipe scripts. [6-7, 9] Errors on $^{15}$N $R_1$ and $R_{1\rho}$ rates were determined using Monte-Carlo simulations and dedicated NMRPipe scripts. [6-7, 9] The error on derived $^{15}$N $R_2$ rates, {$^1$H}-$^{15}$N NOE values and intensity ratios was determined using Gaussian error propagation.

**Fluorescence titrations and data evaluation.** Fluorescence titrations were performed on a Fluorolog-3 fluorimeter (Horiba) at 25°C in buffer A in the presence of 0.5 mM GDPNP, unless indicated otherwise. Binding of FtsY(Bpy) to SecYEG(MDCC) was measured on addition of FtsY(Bpy), monitoring MDCC fluorescence at 460 nm upon excitation at 430 nm.

Binding of FtsY-A207(NBD) to nanodiscs was measured by titrating 0.5 µM nanodiscs with FtsY-A207(NBD). The increase of NBD fluorescence on binding to lipids was measured throughout the emission spectrum upon exciting at 480 nm. The titrations were corrected by subtracting the linear fluorescence increase due to the increase of the FtsY-A207(NBD) concentration measured in parallel in buffer.

Titration curves were evaluated in terms of $K_d$ using a quadratic equation that takes into account the change in the concentration of the added ligand, $P_t$, due to complex formation [11]:

$$F(i) = F_0 + \left(F_{\max} - F_0\right) \cdot 0.5 \cdot \left( (P_t - L_t + K_d) - \sqrt{(P_t - L_t + K_d)^2 - 4P_tL_t} \right) \quad (1)$$

where *F(i)* denotes the fluorescence at point (*i*), $F_0$ the initial fluorescence, $F_{max}$ the final fluorescence level, $P_t$ the total concentration of the fixed ligand, $L_t$ the added ligand concentration, and $K_d$ is the dissociation constant of the complex of *P* and *L*.

## Results

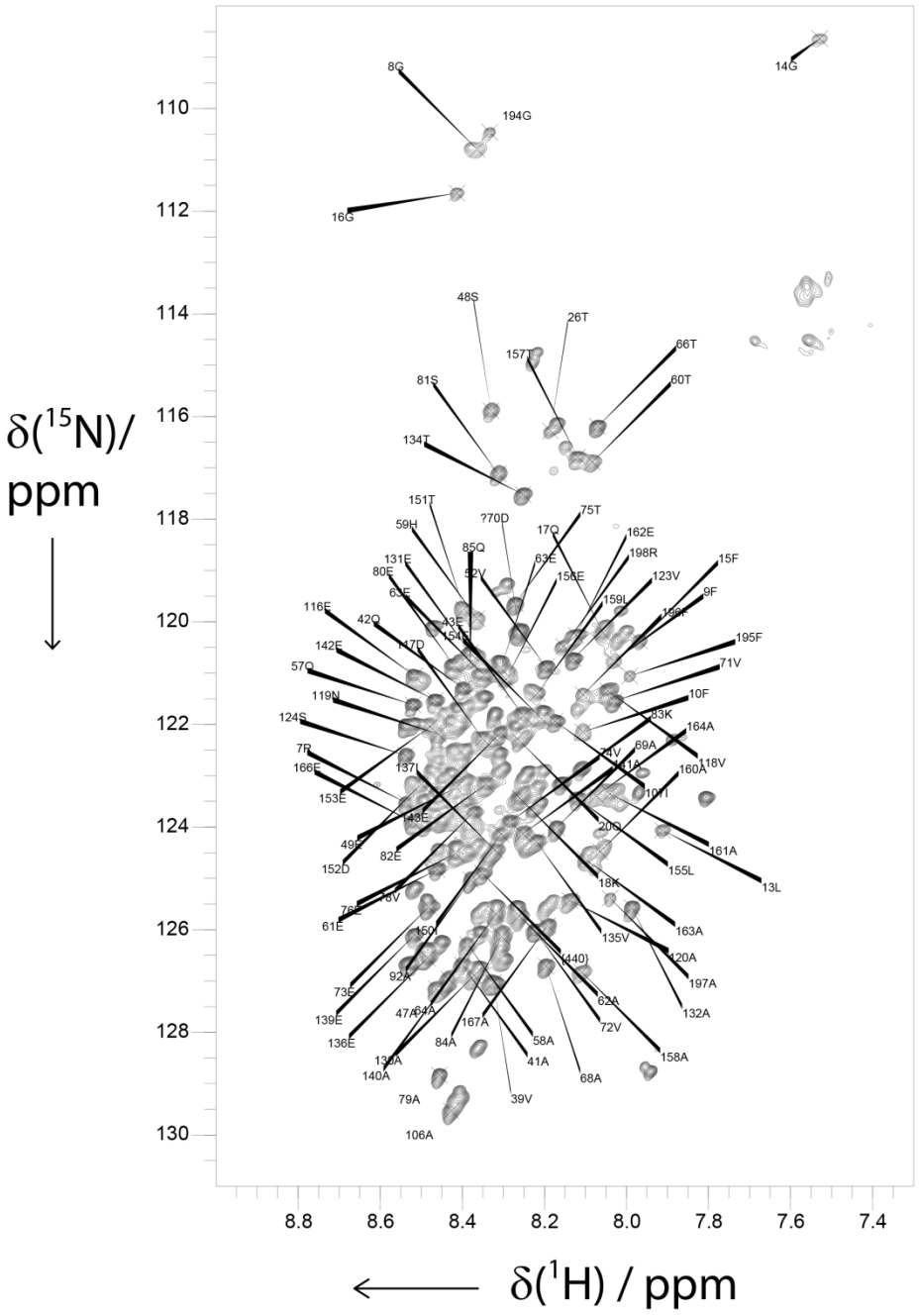


**Figure S1.** Assignment of $^{15}N$-$^{1}H$ 2D TROSY-HSQC spectrum of $^{2}H^{15}N^{13}C$-enriched FtsY-A207. Resonances were assigned as described in Methods.

## Spectral resonance assignment

**Full-length FtsY:**

For full-length FtsY, about 120 out of 474 possible resonances (for 497 amino acids) are visible in $^{1}H^{15}N$ TROSY-HSQC spectra ($^{1}H$ amide proton, $^{15}N$ amide nitrogen Transverse Relaxation Optimized Spectroscopy - Heteronuclear Single Quantum Correlation Spectroscopy) (Figure 1b). The low dispersion of resonances in the proton dimension indicates intrinsic disorder of the visible part of the protein. The comparison of the spectra of FtsY and of the isolated FtsY-A domain (FtsY-A207) confirms that all visible resonances belong to the A domain and resonances of the NG domain are not visible. Apparently, the intrinsically disordered A domain is highly flexible and, therefore, has favorable relaxation properties which result in narrow line widths such that resonances remain visible in the spectra of the full-length protein, although some broadening takes place. By contrast, the tumbling of the structured NG domain appears to be slow, presumably reinforced by low temperature and glycerol in the measuring buffer, leading to line broadening and intensity decrease below the detection threshold. In the spectrum of the full-length protein several resonances are missing that are visible in the spectrum of FtsY-A207. Presumably these resonances belong to residues that are immobilized by intramolecular interactions in the full-length protein.

**FtsY-A207:**

For the construct comprising only the FtsY A domain (FtsY-A207), about 180 out of 190 expected resonances (207 amino acids minus 16 invisible proline residues and the invisible N-terminal amino acid) are visible in two-dimensional $^{15}N^{1}H$-TROSY-HSQC spectra of FtsY-A207 (Fig. 1b, Fig. S1); the remaining resonances either are hidden by spectral overlap or broadened below the detection threshold as the result of dynamic processes on the micro- to millisecond time scale. Out of the visibile resonances, 110 (60%) could be assigned. Further assignments were precluded due to the high abundance of glutamic acid (25%), the presence of repetitive sequences, and close to random-coil chemical shifts. Nevertheless, the assigned resonances cover practically the entire A domain, leaving unassigned only small regions encompassing residues 30–50, 170–182, and 198–207.

**Internal dynamics of FtsY-A207**

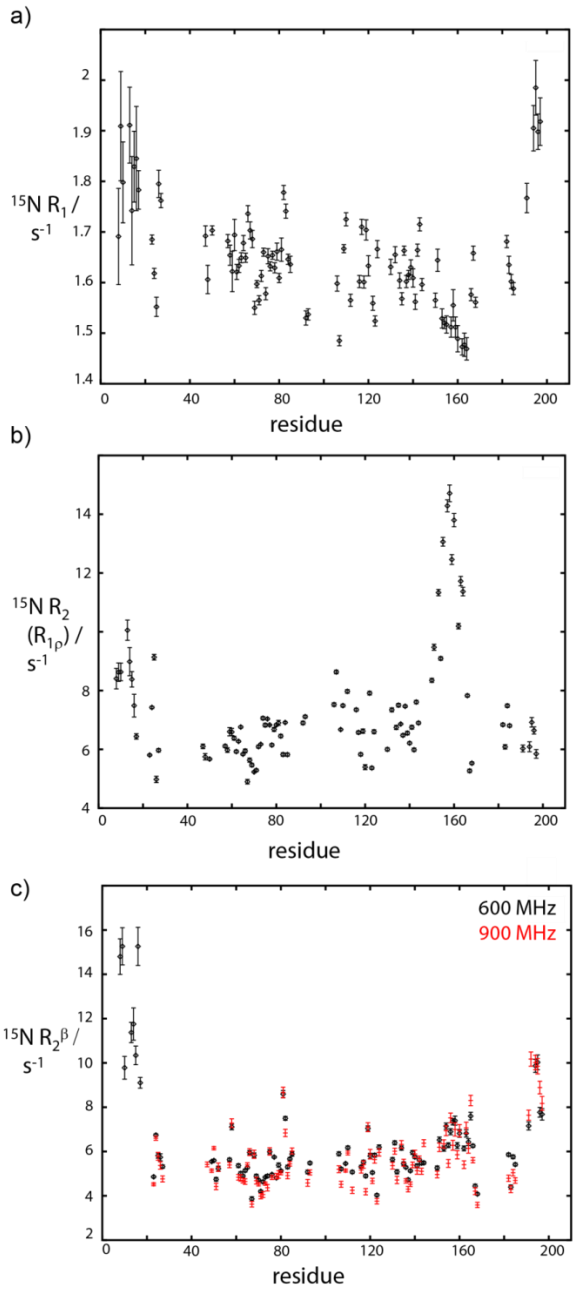


**Figure S2.** $^{15}$N NMR relaxation data on FtsY A207. a) $^{15}$N $R_1$ rates characterize internal protein dynamics on a pico- to nanosecond time scale. b) $^{15}$N $R_2$ rates of assigned resonances as derived from $R_{1\rho}$ rates. c) $^{15}$N $R_2^{\beta}$ rates as measured at 600 MHz (black) or 900 MHz (red) on the slowly relaxing component of the NH doublet.

**Micro-to millisecond dynamics:**

To further characterize the internal dynamics of the A domain we measured $^{15}N\ R_2^{\beta}$ rates in a Hahn-echo based experiment (see above).[8] This observable is sensitive to exchange effects, $R_{ex}$, due to conformational dynamics in the micro- to millisecond time range, and depends on the strength of the magnetic field in a quadratic manner. The central region of the A domain, Ile38 to Ala140, on the average shows low $^{15}N\ R_2^{\beta}$ rates (Figure S2d) which are not increased at 900 MHz compared to 600 MHz. Thus, most of the central part of the A domain does not exhibit extensive conformational dynamics.

## Lipid-binding of FtsY-A207

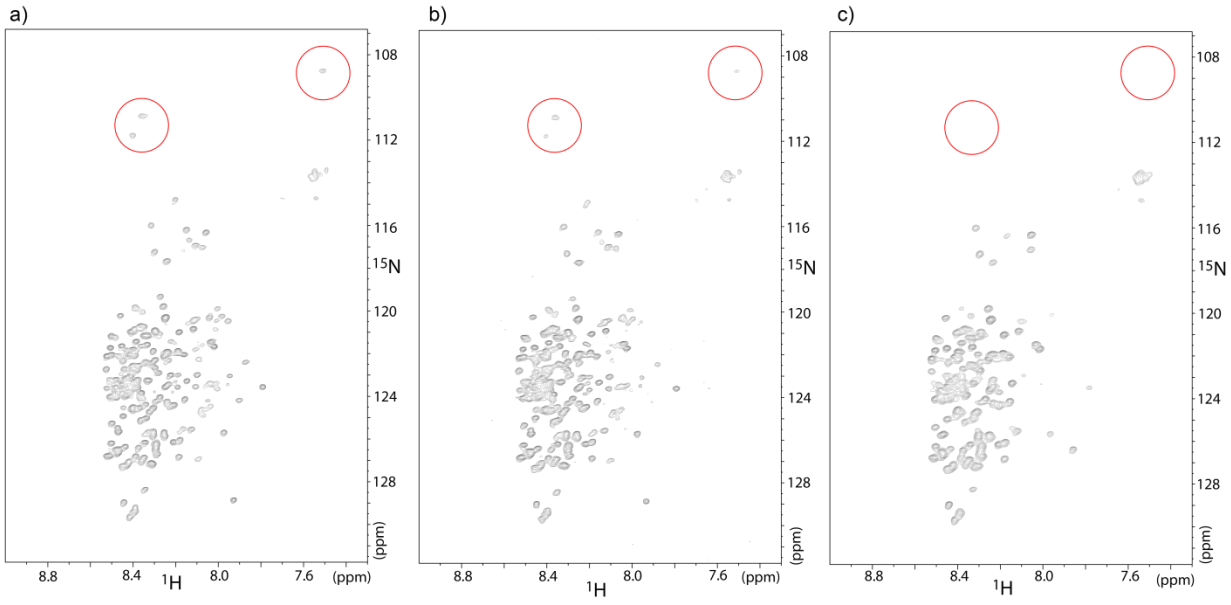


**Figure S3.** Lipid and SecYEG binding of the FtsY A domain. a) $^{15}N$-$^{1}H$ TROSY-HSQC spectra of $^{2}H^{13}C^{15}N$-enriched FtsY-A207 in unbound form, (b) in the presence of lipid nanodiscs and (c) in the presence of SecYEG in nanodiscs. Resonances of Gly residues of the N-terminal region that lose intensity or disappear upon binding to lipids or SecYEG, respectively, are encircled.

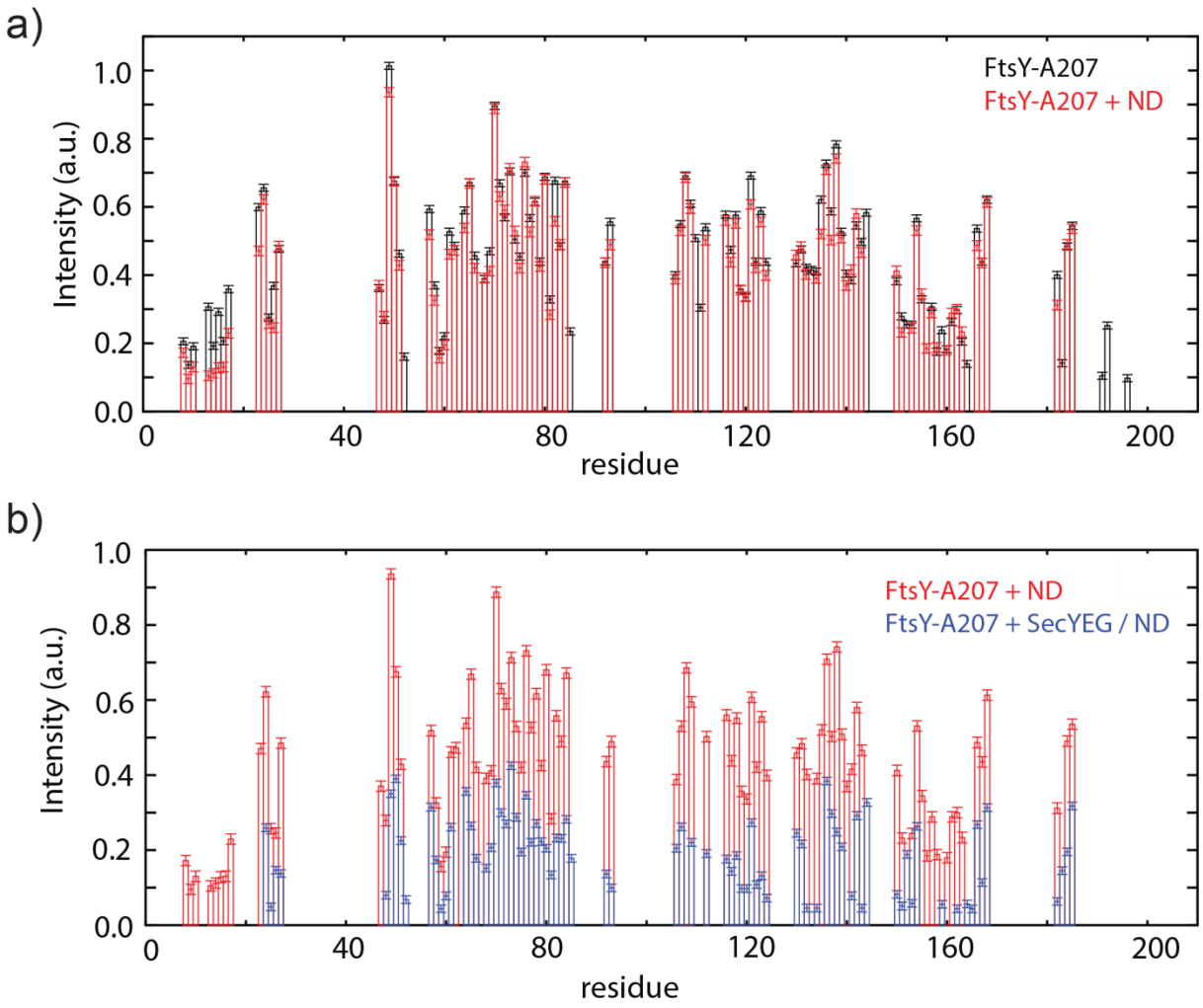


**Figure S4.** Resonance intensities of the $^{15}$N-$^{1}$H TROSY-HSQC spectra from Figure S3. a) Free FtsY-A207 (black bars/symbols) and ND-bound FtsY-A207 (red bars/symbols). b) ND-bound FtsY-A207 (red bars/symbols) and SecYEG-bound FtsY-A207 (blue bars/symbols).

Resonances for the residues 197-207 in the MTS are lacking in the spectra, likely due to helix formation on an intermediate time scale and concomitant intensity decrease below the detection threshold.[12] Consistent with lipid binding of the N terminus of the A domain, a truncated version of FtsY that lacks the N-terminal 14 residues does not bind to membrane lipids, and the exchange of Gly14 with alanine impairs lipid binding of FtsY.[13]

The observed intensity decrease points to an equilibrium between two populations of FtsY-A207, one bound to lipids (not visible by solution NMR) and one unbound (visible by NMR), which are in slow

exchange on the millisecond time scale. As nanodiscs are relatively large with a molecular weight around 150 kDa,[14] FtsY-A207 bound to lipid nanodiscs will adopt the relaxation properties of the latter, which leads to line broadening below the detection threshold. The N terminus of FtsY, which is conserved among enterobacteria, contributes to lipid binding by its positive charge [13] and has a propensity to form an α helix.[15] Our data support these findings, as NMR relaxation data indicate the presence of secondary structure in the N-terminal region already in its unbound form; furthermore, we observe a conformational exchange process in that region which can be attributed to transient α helix formation.

## Electrostatics of FtsY-A207

```
1         10         20         30         40         50         60
MAKEKKRGFF SWLGFGQKEQ TPEKETEVQN EQPVVEEIVQ AQEPVKASEQ AVEEQPQAHT
          70         80         90         100        110        120
EAEAETFAAD VVEVTEQVAE SEKAQPEAEV VAQPEPVVEE TPEPVAIERE ELPLPEDVNA
          130        140        150        160        170        180
EAVSPEEWQA EAETVEIVEA AEEEAAKEEI TDEELETALA AEAAEEAVMV VPPAEEEQPV
          190        200
EEIAQEQEKP TKEGFFARLK RSLLKTK
```

**Figure S5.** Amino acid sequence of the FtsY A domain. Positively charged residues (R,H,K) are colored in light blue, negatively charged residues (D,E) in red, uncharged residues in gray.

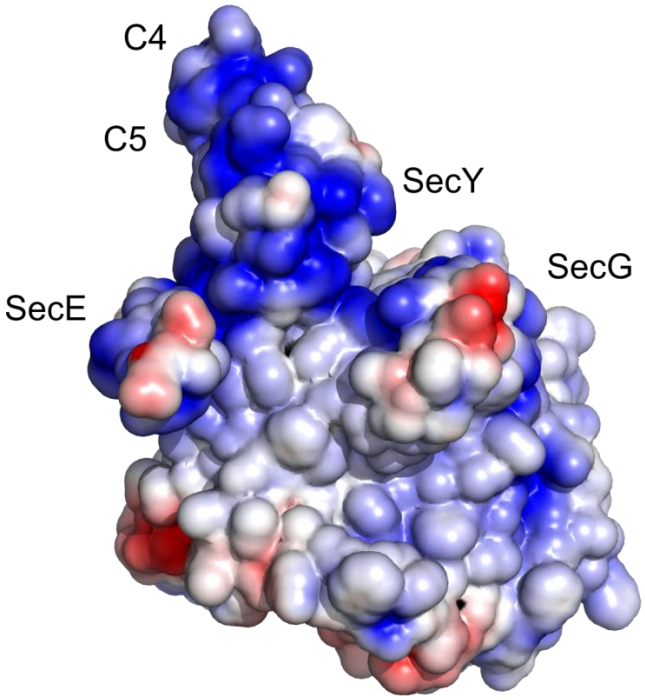


**Figure S6.** Electrostatics of SecYEG. Coloring corresponds to -3 kT/e (red) to +3 kT/e (blue) (see Methods). Calculation of per-atom charge and radii was performed on PDB file 3J45 (only chains Y, E and G were subjected to the calculation) by the PDB2PQB server,[16] applying PARSE force field (continuum electrostatics force field) at pH 7.5. The resulting charge distribution was visualized using the APBS plugin for PyMOL. [17]

## References

[1] L. P. McIntosh, F. W. Dahlquist, *Quarterly reviews of biophysics* **1990**, *23*, 1-38.

[2] Y. Ge, A. Draycheva, T. Bornemann, M. V. Rodnina, W. Wintermeyer, *Nature communications* **2014**, *5*, 5263.

[3] P. Kuhn, A. Draycheva, A. Vogt, N. A. Petriman, L. Sturm, F. Drepper, B. Warscheid, W. Wintermeyer, H. G. Koch, *J Cell Biol* **2015**, *211*, 91-104.

[4] T. H. Bayburt, S. G. Sligar, *FEBS letters* **2010**, *584*, 1721-1727.

[5] R. K. Scopes, *Analytical Biochemistry* **1974**, *59*, 277-282.

[6] K. Pervushin, R. Riek, G. Wider, K. Wuthrich, *Proc Natl Acad Sci U S A* **1997**, *94*, 12366-12371.

[7] F. Delaglio, S. Grzesiek, G. W. Vuister, G. Zhu, J. Pfeifer, A. Bax, *J Biomol NMR* **1995**, *6*, 277-293.

[8] Y. Shen, F. Delaglio, G. Cornilescu, A. Bax, *J Biomol NMR* **2009**, *44*, 213-223.

[9] Y. Wang, O. Jardetzky, *Journal of the American Chemical Society* **2002**, *124*, 14075-14084.

[10] a) N. A. Lakomek, J. Ying, A. Bax, *J Biomol NMR* **2012**, *53*, 209-221; b) N. A. Lakomek, J. D. Kaufman, S. J. Stahl, J. M. Louis, A. Grishaev, P. T. Wingfield, A. Bax, *Angew Chem Int Ed Engl* **2013**, *52*, 3911-3915.

[11] D. M. Jameson, G. Mocz, in *Protein-Ligand Interactions: Methods and Applications* (Ed.: G. Ulrich Nienhaus), Humana Press, Totowa, NJ, **2005**, pp. 301-322.

[12] G. Stjepanovic, K. Kapp, G. Bange, C. Graf, R. Parlitz, K. Wild, M. P. Mayer, I. Sinning, *J Biol Chem* **2011**, *286*, 23489-23497.

[13] B. Weiche, J. Burk, S. Angelini, E. Schiltz, J. O. Thumfart, H. G. Koch, *J Mol Biol* **2008**, *377*, 761-773.

[14] F. Hagn, M. Etzkorn, T. Raschle, G. Wagner, *Journal of the American Chemical Society* **2013**, *135*, 1919-1925.

[15] D. Braig, C. Bar, J. O. Thumfart, H. G. Koch, *J Mol Biol* **2009**, *390*, 401-413.

[16] a) T. J. Dolinsky, P. Czodrowski, H. Li, J. E. Nielsen, J. H. Jensen, G. Klebe, N. A. Baker, *Nucleic acids research* **2007**, *35*, W522-555; b) T. J. Dolinsky, J. E. Nielsen, J. A. McCammon, N. A. Baker, *Nucleic acids research* **2004**, *32*, W665-667.

[17] N. A. Baker, D. Sept, S. Joseph, M. J. Holst, J. A. McCammon, *Proc Natl Acad Sci U S A* **2001**, *98*, 10037-10041.

| Residue number | AA | $\delta(^{1}H)$ [a] [ppm] | $\delta(^{15}N)$ [a] [ppm] | $\delta(^{13}C'_{i-1})$ [ppm] | $\delta(C^{\alpha})$ [b] [ppm] | $\delta(C^{\beta})$ [b] [ppm] |
|---|---|---|---|---|---|---|
| 8 | G | 8.4 | 110.8 | 175.3 | 44.5 | n |
| 9 | F | 8.0 | 120.8 | 177.2 | 57.5 | n |
| 10 | F | 8.1 | 122.2 | n | 57.1 | n |
| 13 | L | 7.9 | 124.1 | 179.3 | 54.8 | n |
| 14 | G | 7.5 | 108.7 | 175.6 | 44.4 | n |
| 15 | F | 8.0 | 120.4 | 178.4 | 57.8 | n |
| 16 | G | 8.4 | 111.7 | 175.8 | 44.7 | n |
| 17 | Q | 8.1 | 120.2 | n | 55.3 | 29.6 |
| 23 | E | 8.5 | 122.0 | 179.2 | 56.2 | 29.3 |
| 24 | K | 8.4 | 121.9 | 178.7 | 56.3 | 29.5 |
| 25 | E | 8.3 | 122.3 | 178.6 | 56.2 | 29.3 |
| 26 | T | 8.2 | 116.3 | 176.3 | 61.7 | 69.2 |
| 27 | E | 8.4 | 124.5 | n | 55.9 | 29.5 |
| 47 | A | 8.5 | 127.2 | 179.9 | 52.2 | 18.4 |
| 48 | S | 8.3 | 115.9 | 178.1 | 58.1 | 63.5 |
| 49 | E | 8.4 | 123.3 | 178.1 | 56.0 | 29.6 |
| 50 | Q | 8.4 | 123.4 | 178.3 | 55.9 | 29.5 |
| 51 | A | 8.3 | 125.6 | 179.6 | 52.0 | 18.4 |
| 52 | V | 8.0 | 120.4 | n | 61.7 | 31.8 |
| 57 | Q | 8.5 | 121.6 | 177.6 | 55.0 | 28.7 |
| 58 | A | 8.4 | 126.3 | 179.4 | 52.0 | 18.5 |
| 59 | H | 8.4 | 120.0 | 177.3 | 55.7 | 29.9 |
| 60 | T | 8.1 | 116.9 | 176.2 | 61.2 | 69.4 |
| 61 | E | 8.5 | 124.0 | 178.3 | 55.7 | 29.5 |
| 62 | A | 8.3 | 125.7 | 179.8 | 52.1 | 18.4 |
| 63 | E | 8.3 | 120.9 | 178.2 | 55.9 | 29.4 |
| 64 | A | 8.3 | 125.7 | 179.8 | 52.1 | 18.4 |
| 65 | E | 8.3 | 121.1 | 178.5 | 56.1 | 29.4 |
| 66 | T | 8.1 | 116.2 | 175.9 | 61.3 | 69.4 |
| 67 | F | 8.2 | 123.3 | 177.2 | 57.1 | 38.9 |
| 68 | A | 8.2 | 126.7 | 178.9 | 51.8 | 18.5 |
| 69 | A | 8.2 | 124.0 | 179.4 | 51.8 | 18.5 |
| 70 | D | 8.3 | 120.2 | 178.0 | 53.9 | 40.3 |
| 71 | V | 8.0 | 121.6 | 178.1 | 61.8 | 31.9 |
| 72 | V | 8.2 | 126.0 | 178.2 | 61.7 | 32.0 |
| 73 | E | 8.5 | 125.6 | 178.1 | 55.8 | 29.5 |
| 74 | V | 8.3 | 123.9 | 178.2 | 61.8 | 31.8 |
| 75 | T | 8.3 | 119.7 | 176.3 | 61.4 | 69.2 |
| 76 | E | 8.4 | 124.4 | 178.0 | 56.0 | 29.5 |
| 77 | Q | 8.4 | 123.4 | 178.0 | 56.0 | 29.6 |
| 78 | V | 8.4 | 123.7 | 177.9 | 61.8 | 31.9 |
| 79 | A | 8.5 | 128.9 | 179.1 | 52.0 | 18.4 |
| 80 | E | 8.4 | 120.9 | 178.8 | 56.4 | 29.4 |

| | | | | | | |
|---|---|---|---|---|---|---|
| 81 | S | 8.3 | 117.1 | 177.8 | 58.4 | 63.6 |
| 82 | E | 8.3 | 123.2 | 178.3 | 55.9 | 29.2 |
| 83 | K | 8.2 | 123.2 | 178.2 | 55.4 | 32.1 |
| 84 | A | 8.3 | 126.2 | 179.6 | 52.0 | 18.3 |
| 85 | Q | 8.4 | 120.8 | n | 55.3 | 28.8 |
| 92 | A | 8.4 | 125.1 | 179.9 | 51.9 | 18.5 |
| 93 | Q | 8.4 | 121.3 | n | 56.1 | 29.5 |
| 106 | A | 8.4 | 129.6 | 179.3 | 51.7 | 18.3 |
| 107 | I | 8.2 | 121.9 | 178.2 | 60.4 | 38.0 |
| 108 | E | 8.5 | 126.4 | 177.8 | 55.8 | 29.6 |
| 109 | R | 8.4 | 123.0 | 176.2 | 55.8 | 29.4 |
| 110 | E | 8.5 | 123.2 | 178.4 | 56.2 | 28.9 |
| 111 | E | 8.4 | 121.7 | 177.9 | 55.3 | 29.5 |
| 112 | L | 8.4 | 126.1 | n | 52.5 | 40.5 |
| 116 | E | 8.5 | 121.1 | 178.2 | 56.1 | 29.4 |
| 117 | D | 8.4 | 122.3 | 178.4 | 53.7 | 40.4 |
| 118 | V | 8.0 | 121.4 | 177.9 | 62.1 | 31.8 |
| 119 | N | 8.5 | 122.2 | 176.9 | 52.7 | 38.2 |
| 120 | A | 8.1 | 125.4 | 179.9 | 52.4 | 18.3 |
| 121 | E | 8.3 | 120.9 | 177.9 | 55.9 | 29.5 |
| 122 | A | 8.4 | 126.7 | 179.4 | 51.8 | 18.4 |
| 123 | V | 8.1 | 120.7 | 178.1 | 61.4 | 32.2 |
| 124 | S | 8.5 | 122.6 | n | 56.0 | 63.1 |
| 130 | A | 8.4 | 126.9 | 179.4 | 51.8 | 18.4 |
| 131 | E | 8.4 | 120.6 | 176.7 | 54.8 | 28.8 |
| 132 | A | 8.0 | 125.6 | 179.8 | 52.1 | 18.3 |
| 133 | E | 8.4 | 120.8 | 178.5 | 55.9 | 29.5 |
| 134 | T | 8.3 | 117.5 | 176.1 | 61.5 | 69.3 |
| 135 | V | 8.2 | 124.3 | 177.8 | 61.6 | 32.1 |
| 136 | E | 8.5 | 126.5 | 177.9 | 55.8 | 29.6 |
| 137 | I | 8.3 | 124.5 | 178.1 | 60.5 | 37.6 |
| 138 | V | 8.3 | 127.1 | 177.9 | 61.7 | 31.9 |
| 139 | E | 8.5 | 126.1 | 177.4 | 55.0 | 28.6 |
| 140 | A | 8.4 | 127.0 | 178.5 | 52.2 | 18.4 |
| 141 | A | 8.3 | 124.2 | 179.9 | 51.9 | 18.2 |
| 142 | E | 8.5 | 121.5 | 178.8 | 56.4 | 29.3 |
| 143 | E | 8.3 | 122.2 | 178.4 | 56.2 | 29.4 |
| 144 | E | 8.4 | 121.8 | n | 55.2 | 28.9 |
| 150 | I | 8.3 | 124.2 | 178.3 | 60.4 | 37.6 |
| 151 | T | 8.4 | 119.8 | 176.2 | 61.0 | 69.8 |
| 152 | D | 8.5 | 123.2 | 178.9 | 54.7 | 40.1 |
| 153 | E | 8.5 | 122.0 | 178.9 | 57.5 | 29.3 |
| 154 | E | 8.2 | 121.9 | 179.7 | 57.2 | 29.1 |
| 155 | L | 8.1 | 123.5 | 180.0 | 55.9 | 41.1 |
| 156 | E | 8.3 | 121.1 | 180.0 | 57.4 | 28.9 |
| 157 | T | 8.1 | 116.8 | 177.2 | 63.3 | 68.8 |
| 158 | A | 8.1 | 126.8 | 180.9 | 53.2 | 17.9 |

| | | | | | | |
|---|---|---|---|---|---|---|
| 159 | L | 8.2 | 121.4 | 180.4 | 55.6 | 41.0 |
| 160 | A | 8.1 | 124.5 | 180.4 | 52.7 | 17.9 |
| 161 | A | 8.0 | 123.3 | 180.7 | 52.7 | 17.8 |
| 162 | E | 8.1 | 120.3 | 178.9 | 56.7 | 29.2 |
| 163 | A | 8.1 | 124.6 | 180.0 | 52.3 | 17.9 |
| 164 | A | 8.1 | 123.4 | 175.8 | 52.3 | 18.1 |
| 165 | E | 8.0 | 120.1 | 178.0 | 55.7 | 29.6 |
| 166 | E | 8.5 | 123.9 | 178.1 | 55.7 | 29.6 |
| 167 | A | 8.2 | 126.0 | 179.6 | 51.9 | 18.4 |
| 168 | V | 8.2 | 120.9 n | | 61.7 | 32.0 |
| 182 | E | 8.4 | 122.6 | 178.2 | 55.9 | 29.5 |
| 183 | I | 8.2 | 123.7 | 177.8 | 60.5 | 37.8 |
| 184 | A | 8.4 | 129.3 | 179.5 | 51.9 | 18.3 |
| 185 | Q | 8.3 | 121.5 n | | 56.1 | 29.5 |
| 191 | T | 8.2 | 115.0 | 176.7 | 61.1 | 69.6 |
| 192 | K | 8.4 | 123.9 n | | 56.0 | 32.0 |
| 194 | G | 8.3 | 110.5 | 175.9 | 44.7 n | |
| 195 | F | 8.0 | 121.1 | 177.7 | 58.2 | 38.8 |
| 196 | F | 8.1 | 121.4 | 177.4 | 57.6 | 38.7 |
| 197 | A | 8.0 | 125.4 | 179.4 | 52.3 | 18.4 |

[a] Spectral resonance positions for the slowly relaxing NH doublet („TROSY“) component are shown, as

[b] Raw experimental data are presented (before isotope shift correction).